PHYSICAL REVIEW B VOLUME 12, NUMBER 6 15 SEPTEMBER 1975

Transport property of zero-gap semiconductors under tensile stress*

L. Liu
Department of Physics, Northwestern University, Evanston, Illinois 60201

W. Leung
Department of Physics, Northwestern University, Evanston, Illinois 60201
and Department of Physics,† *Imperial College of Science and Technology, London, United Kingdom*
(Received 19 May 1975)

The band structure of symmetry-induced zero-gap semiconductors under uniaxial tensile stress is studied. It is found that there exist regions in the reciprocal space where one component of the effective-mass tensor of either electrons or holes becomes negative. In particular, the anomalous region for holes can be made sufficiently large to allow for the occurrence of negative-differential-resistance (NDR) effect. The *I*-*V* characteristics for *p*-type α-Sn and HgTe at both zero temperature and finite temperature (4.2 and 77°K) are obtained by simple transport calculations. From these calculated *I*-*V* characteristics, one gets some idea about the sample requirements and magnitude of stress needed for NDR effect.

I. INTRODUCTION

For semiconductors like α-Sn or HgTe, the conduction band makes contact with the valence band at one point in the reciprocal space, and hence the energy gap is identically zero. The band-edge point, i.e., the contact point, is a degenerate quantum state, and the corresponding wave functions belong to a multidimensional irreducible representation of the symmetry group of the crystal. In other words, the degeneracy of the band edge is required by symmetry. At the beginning, the zero-gap model was proposed for α-Sn.[1] Later on, several compound semiconductors like HgTe,[2] HgSe,[3] HgS,[4] and Cd_3As_2,[5] were reported to possess similar band-edge structure. As the list of symmetry-induced zero-gap semiconductors grows, so does the interest in investigating their properties, both theoretically and experimentally.

Since the degeneracy of the band edge is symmetry induced, the band-edge structure can be significantly distorted by applying symmetry-breaking fields such as uniaxial stress, which destroys the original cubic symmetry of the sample. For α-Sn, it has been shown experimentally that compressional uniaxial stress[6] will open up an energy gap by pulling the conduction and the valence band apart while tensile stress[7] will cause band overlap. Let us consider the case of tensile stress here. Under tensile stress, the conduction band for $\vec{k}$ along the stress direction will move downward in energy relative to the valence band, and intersect it at points away from their original contact point, i.e., the center of the Brillouin zone. Thus, part of the original conduction band will be pulled down in energy to form a segment of the new valence band. Correspondingly, one segment of the original valence band will be moved up in energy and become part of the conduction band under stress. This interchange of roles between the conduction and the valence bands would make the effective mass of the charge carriers negative. Therefore, when charge carriers, electrons, or holes, are transferred into the negative-mass region, say, by an external electric field, their masses undergo a change in sign and magnitude. This makes it interesting to study the electronic transport properties for such a system. Especially, a negative-differential-resistance (NDR) effect[8,9] is expected to occur, which may have important practical applications.

We limit ourselves to the consideration of motion of holes in this paper. The reason is that only the valence-band structure under tensile stress is capable of producing NDR effect. Although the conduction-band structure is also anomalous, the anomalous region is too small to produce any appreciable non-Ohmic effect. We do a transport calculation specifically for α-Sn and HgTe, whose band parameters are better known among all the existing zero-gap semiconductors. The transport calculation is first done at zero temperature to demonstrate the existence of the NDR effect at low temperature and then extended to finite temperature to see how temperature would affect it.

In Sec. II we discuss the band-edge structure of zero-gap semiconductors under uniaxial tensile stress. The transport calculation is described in Sec. III for the zero-temperature case and in Sec. IV for the finite-temperature case. In Sec. V we discuss some related NDR-producing phenomena, and finally, in Sec. VI questions related to the oversimplified assumptions made in the present paper are discussed.

II. BAND-EDGE STRUCTURE

The band-edge structure for zero-gap semiconductors can be best appreciated by comparing that

of α-Sn with the well-known band structure of Ge near the center of the Brillouin zone, i.e., the Γ point. A sketch of such band structures is presented in Fig. 1, which also includes a band scheme for the compound semiconductor InSb. In going from Ge to α-Sn, the order of the Γ_8^+ and Γ_7^- bands is reversed. This level crossing causes the light-hole band in Ge to invert its curvature and become the conduction band in α-Sn. Thus, the conduction band touches the valence band at the Γ_8^+ point in α-Sn, and the energy gap becomes identically zero. For compound zero-gap semiconductors, apart from some insignificant features caused by the lack of inversion symmetry, the band-edge structure is essentially the same as that of α-Sn. As the Γ_8^+ state is the valence-band edge for Ge, it has been well studied ever since the days of the early cyclotron resonance investigations.[10] Thus, we have the advantage of applying the well-known hole structure for Ge to the band edge of zero-gap semiconductors, with only minor modifications. For example, the band edge of zero-gap semiconductors is represented by the following expression:

$$E(\vec{k}) = Ak^2 \pm [B^2k^4 - C^2(k_x^2k_y^2 + k_y^2k_z^2 + k_z^2k_x^2)]^{1/2}, \qquad (2.1)$$

where the plus sign applies to the conduction band and the minus sign the valence band. Comparing with the expression applied to the light-hole and heavy-hole bands of Ge,[10] we have only changed the sign of the warping term. Of course, the band parameters A, B, and C now should assume a different set of values from that for Ge. The band parameters for α-Sn and HgTe are given in Table I.

The valence-band-edge structure for Ge under uniaxial stress is also a well-studied subject.[11,12] We can extend these well-known results to zero-gap semiconductors with Γ_8^+ band edge. We shall consider two cases, one with (0, 0, 1) stress and one with (1, 1, 1) stress.

A. (0,0,1) tensile stress

Under (0, 0, 1) tensile stress the form of the conduction and the valence band near the band edge becomes

$$E_{c,v}(\vec{k}) = Ak^2 \pm \{B^2k^4 - C^2[k_\parallel^2k_\perp^2 + \tfrac{1}{8}k_\perp^4(1-\cos 4\Phi)] + \Delta_0^2 - B\Delta_0(2k_\parallel^2 - k_\perp^2)\}^{1/2}, \qquad (2.2)$$

where the plus sign gives the conduction-band and the minus sign the valence-band structure. The wave vectors $k_\parallel$ and $k_\perp$ refer to the parallel and perpendicular component of $\vec{k}$ with respect to the stress axis, respectively. The azimuthal angle Φ is defined with respect to a cubic axis in the plane perpendicular to the stress direction. The parameter Δ_0 is half of the energy separation between the conduction and the valence band at $\vec{k}=0$; its actual value depends on the magnitude of the applied stress

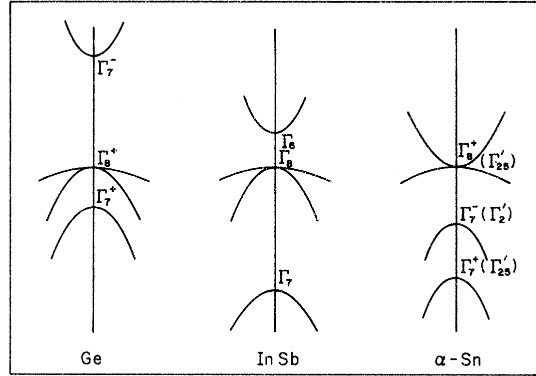

FIG. 1. Sketch of the energy-band structure of Ge, InSb, and α-Sn near the center of the Brillouin zone.

and the deformation potential of the material. Based on experiments done with α-Sn,[6,7] the sign of Δ_0 is positive. In Eq. (2.2) the identical energy shifts of the two bands due to the hydrostatic component of the stress has been neglected.

As given in Table I, the band parameters for α-Sn and HgTe are rather similar. Therefore, we shall use only α-Sn to illustrate the band-edge structure under uniaxial tensile stress in this section. The E vs $k_\parallel$ relationship for α-Sn at $k_\perp=0$ is sketched in Fig. 2 by assigning a value of 15 meV to Δ_0. The drawing shows clearly the crossing of the two bands at $k_\parallel = \pm\sqrt{\Delta_0/B}$ when stress is applied. Let us look at the region between the two crossing points. There is a segment in the lower band which, unlike the rest of the band, has a positive curvature. This curvature actually is identical to that of the original conduction band before stress is applied. In terms of the effective mass along the stress direction, this means that holes in this anomalous region possess negative mass equal to the electron mass in magnitude. Similarly, the upper band has a segment between the crossing points with negative curvature equal to that of the original valence band. Hence electrons in this anomalous region also become negative-mass carriers with the magnitude of its mass equal to that of the normal holes.

The band structure of the $k_\perp=0$ plane is different from that described above. Now, there is no contact between the conduction and the valence band and a finite-energy gap exists. However, we still have an anomalous region for the lower E vs $k_\parallel$ band so long as the $k_\perp$ value is not too large. The anomalous structure for the upper band, however, disappears much faster as the $k_\perp$ value increases. This makes the conduction band a poor candidate for producing NDR effect. These band-edge structures for the $k_\perp \neq 0$ plane are also shown in Fig. 2 (with $\Phi=0$). Thus, the electronic structure under

TABLE I. Band parameters in atomic units.

	A	B	C^2
α-Sn[a]	15.0	22.9	696
HgTe[b]	18.3	22.3	294

[a]W. Leung and L. Liu, Phys. Rev. B 7, 718 (1973).
[b]W. Zawadzki and J. Kowalski, Solid State Commun. 15, 303 (1974).

uniaxial tensile stress is again with identically zero-energy gap. But now the valence band makes contact with the conduction band at two points in-

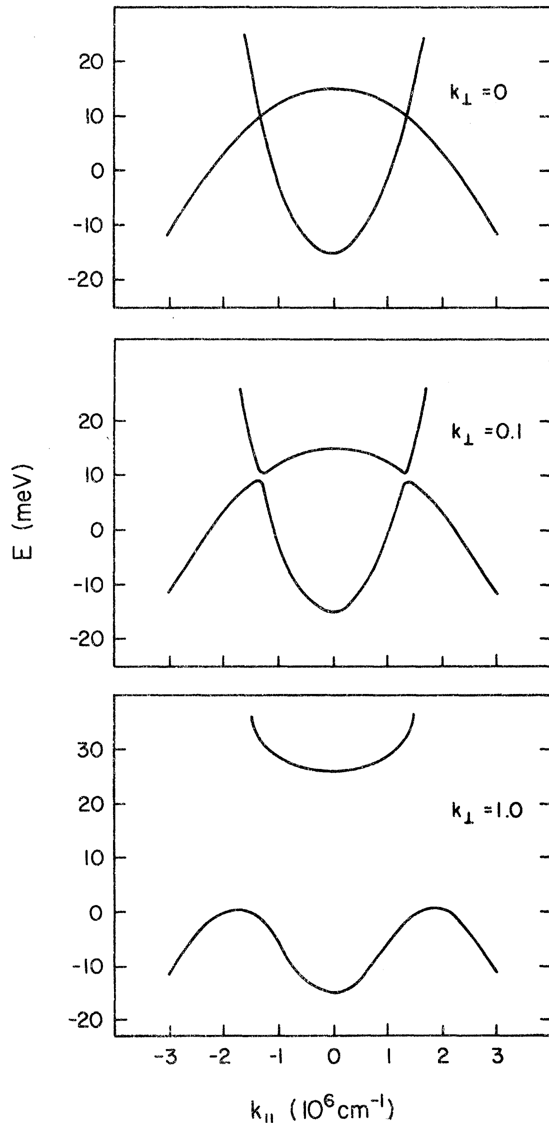

FIG. 2. Energy-band structure of α-Sn under (0, 0, 1) tensile stress. The band splitting parameter Δ_0 is taken to be 15 meV, which can be produced by a stress of about 2×10^9 dyn/cm^2.

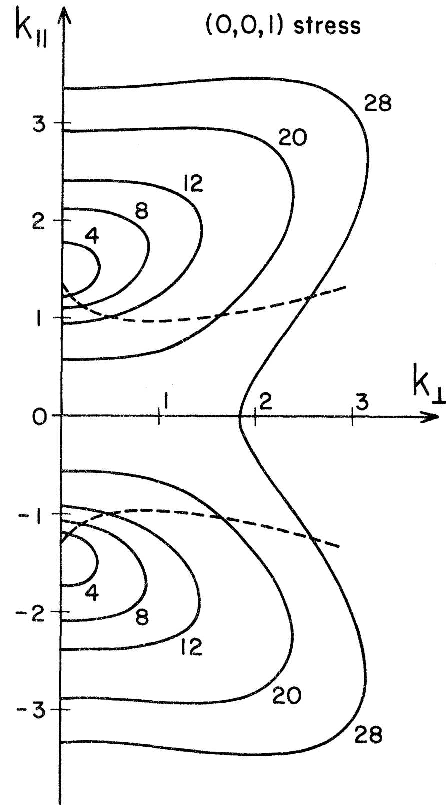

FIG. 3. Constant-energy contour for holes in α-Sn under (0, 0, 1) tensile stress. The parameter Δ_0 is taken to be 15 meV. The wave vectors $k_\parallel$ and $k_\perp$ are expressed in units of 10^6 cm^{-1}, and the energy associated with each contour in meV measured downward from the valance-band maxima. The region between the dotted lines is where the hole mass becomes negative.

stead of one in the no-stress case; these are the crossing points with $(k_\parallel, k_\perp)$ coordinates given by $(\pm\sqrt{\Delta_0/B}, 0)$ as mentioned previously.

A better way to appreciate the electronic structure is to study the constant-energy surfaces. We shall confine ourselves to the hole surfaces only. From Eq. (2.2), it is seen that the constant-energy surfaces should have fourfold symmetry around the stress axis as indicated by the $\cos 4\Phi$ term in the energy expression. This Φ dependence is, however, rather weak at small energies for α-Sn or HgTe. For example, for α-Sn, at an energy of 8 meV as measured downward from the valence-band maxima and a fixed $k_\parallel$, the deviation of $k_\perp$ from its mean value does not exceed 1%. Therefore, we shall neglect the Φ dependence henceforth. The constant-energy contour for the valence band in a $k_\parallel$-$k_\perp$ plane is shown in Fig. 3. Since full axial symmetry around the stress axis is now assumed, the constant-energy surfaces may be obtained by rotating the drawing around the $k_\parallel$ axis. It is seen

that for small energies ($\ll 2\Delta_0$) as measured downward from the two valence-band maxima, the constant-energy surfaces are approximately two disconnected ellipsoids compressed along the stress direction. As the energy increases, the two separate pieces gradually join up with each other. The region where the mass component of the hole along the stress direction becomes negative is also indicated in Fig. 3.

For our later use, we also evaluate numerically the number of holes contained within a given Fermi surface. This is easily done, especially when the surface is assumed to possess axial symmetry. The result is shown in Fig. 4. In the small energy region shown, the density of holes is found to be proportional to the cubic power of the Fermi energy. This result can be appreciated qualitatively as in the following: As we have seen, for small energies the constant-energy surfaces are approximately ellipsoids. If we study the dependence of the three axes of the ellipsoid on the energy, we find that each one is proportional to the first power in energy. Hence, the volume of the ellipsoid is dependent on the energy to the cubic power.

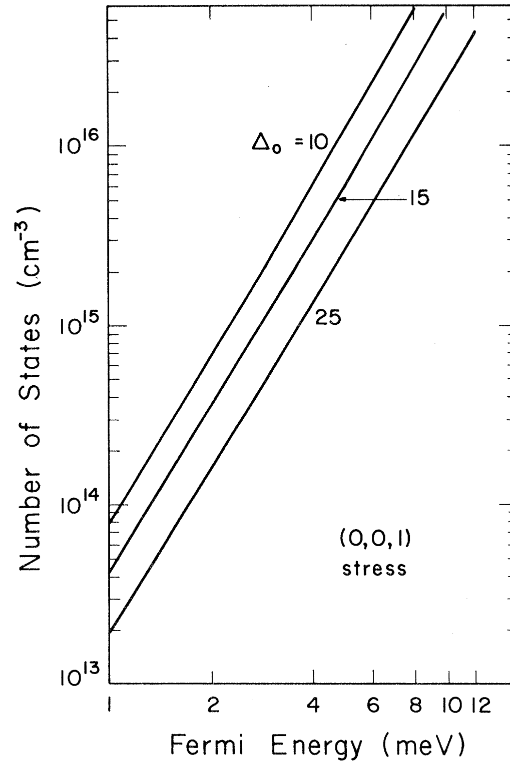

FIG. 4. Number of holes in α-Sn contained within a given Fermi surface. It is noted that the carrier number is approximately proportional to E_F^3 within the Fermi energy range shown here.

B. (1,1,1) tensile stress

In this case, the energy expression for the two bands becomes

$$E_{c,v}(\vec{k}) = Ak^2 \pm [B^2k^4 - C^2(\tfrac{1}{3}k_\parallel^4 + \tfrac{1}{4}k_\perp^4 - \tfrac{1}{3}\sqrt{2}\,k_\perp^3 k_\parallel \sin 3\Phi) + \Delta_0^2 - (B^2 - \tfrac{1}{3}C^2)^{1/2}\Delta_0(2k_\parallel^2 - k_\perp^2)]^{1/2} \qquad (2.3)$$

if we neglect the energy shift due to the hydrostatic component of the stress. Here, the azimuthal angle Φ refers to a coordinate system in which $\hat{k}_z$ is along (1, 1, 1) and $\hat{k}_x$ along $(1, \bar{1}, 0)$. Now, the constant-energy surfaces should possess threefold symmetry around the stress axis. Again, we assume perfect axial symmetry, and plot the constant-energy contours in Fig. 5, which also shows the negative-mass region. For small energies, the constant-energy surfaces are approximately disconnected ellipsoids as in the (0, 0, 1) stress case, but now the ellipsoidal axis is elongated instead of being compressed along the stress axis. For $\Delta_0 = 15$ meV, the anomalous region ceases to exist for $k_\perp$ values beyond approximately 2.1×10^6 cm^{-1}. The number of states contained within a given energy surface is calculated and shown in Fig. 6. As in the (0, 0, 1) stress case, an E^3 dependence is found for small values of E.

A brief discussion of the band structure under tensile stress has been published elsewhere.[13]

C. Compressional stress

The compressional stress is not the topic of this paper. We mention it only to show later why zero-gap semiconductors under compressional stress are not expected to show NDR effect even though there also exists a negative-mass region for holes in the band structure.

The band structure for α-Sn under compressional stress has been investigated theoretically by Cardona[14] and experimentally by Roman and Ewald.[6] As mentioned previously, the conduction and valence bands are pulled apart, and an energy gap is opened up by the compressional stress. The maximum of the valence band is shifted from the original band-edge point (Γ_8^+ state) along a direction perpendicular to the stress axis. Thus, the new maxima may be situated along a ring around the stress axis and the constant-energy surfaces for holes become toroidal in shape. The region near the center of the toroidal surface is an anomalous region in which the hole-mass component along a direction perpendicular to the stress axis becomes negative. On the other hand, the conduction band is normal in the sense that the band minimum stays at the center of the Brillouin zone (BZ), and no negative-mass region for electrons occurs.

From the summary of Cardona's results above, we see that the electronic structure of zero-gap

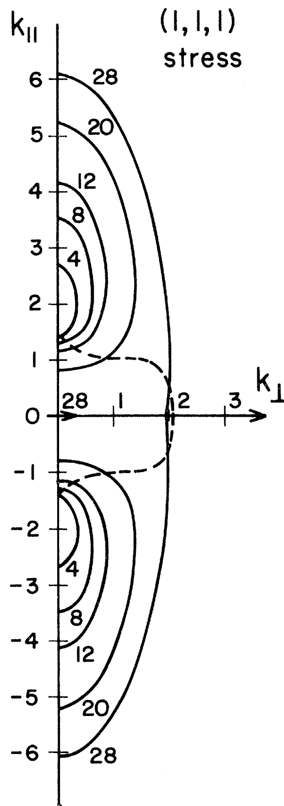

FIG. 5. Constant-energy contour for holes in α-Sn under (1, 1, 1) tensile stress. The parameter Δ_0 is taken to be 15 meV. The units used are the same as in Fig. 3. The boundary of the negative-mass region is marked by dashed lines.

to current opposite in direction to that due to normal carriers, the total current in the sample may actually decrease as more and more carriers are transferred into the anomalous region under increasing values of the electric field. When the electric field is increased further, however, both ellipsoids may be transferred out of the anomalous region and then Ohmic behavior should resume. In the qualitative considerations above we are tacitly assuming that the sharp boundary of the Fermi surface is not distorted to any large extent by the electric field, which only drives the hole ellipsoids away from their positions at equilibrium. To study the NDR effect quantitatively, we must know how the equilibrium distribution function is distorted by the electric field.

To simplify the calculation of the steady-state distribution function in the presence of an electric field, we have to make certain assumptions. We assume that neither the scattering mechanisms nor the electric field cause any interband transitions. Therefore, if we start with a p-type sample at zero temperature, the carriers would always stay in the valence band. With a relaxation-time ansatz, we can then solve the following Boltzmann equation to obtain the steady-state distribution function f for holes:

semiconductors under compressional stress is very different from that under tensile stress.

III. NDR EFFECT AT ZERO TEMPERATURE

Before we make a transport calculation to show the existence of NDR effect, we shall first use qualitative reasonings to indicate why this effect may occur at low temperature. Let us take as an example a p-type sample at absolute-zero temperature. If the hole concentration is small, corresponding to a small Fermi energy ($\ll 2\Delta_0$) of, say 4 meV, the Fermi surface consists of two ellipsoids as shown in Fig. 3. At equilibrium, all the holes are contained within these two ellipsoids. As one can see from the figure, only a very small fraction of the holes are anomalous. With an electric field applied along the stress direction, the distribution function is distorted along this direction in such a way that one of the ellipsoids is moved into the negative-mass region and the other is moved away from it. Hence when steady state is established by the scattering mechanisms, a larger fraction of the hole carriers becomes anomalous. According to the discussion in Sec. II, these anomalous carriers are much lighter (about ten times lighter) than the normal carriers on the average. Since carriers with negative mass should give rise

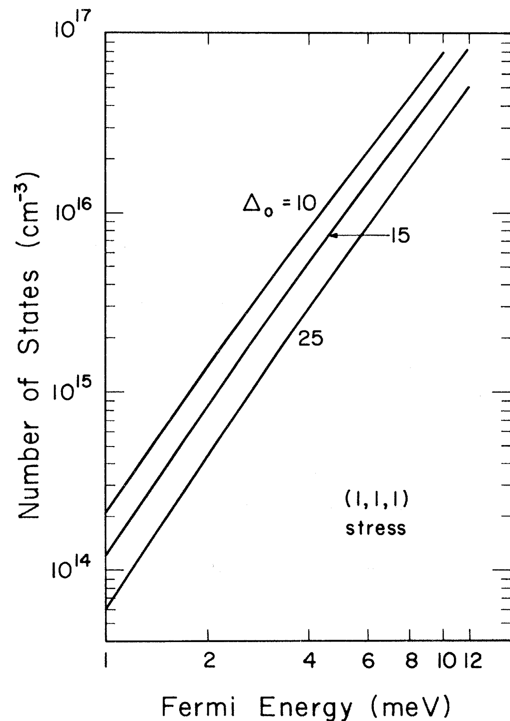

FIG. 6. Number of holes in α-Sn contained within a Fermi surface. The $E_F^{3/2}$ dependence is also true for (1, 1, 1) stress.

$$\frac{eF}{\hbar}\frac{\partial f}{\partial k_\parallel}=-\frac{f-f^0}{\tau}, \tag{3.1}$$

where F is the electric field strength applied along the stress axis and f^0 is the equilibrium distribution function for holes. If we further assume that the relaxation time τ is isotropic and a constant, we can easily find out the one-dimensional Green's function for Eq. (3.1) as follows:

$$G(k'_\parallel, k_\parallel)=a^{-1}\exp[-(k_\parallel-k'_\parallel)/a]\times\begin{cases}[\exp(K/a)-1]^{-1}, & k_\parallel<k'_\parallel\\ [1-\exp(-K/a)]^{-1}, & k_\parallel>k'_\parallel\end{cases}, \tag{3.2}$$

where K is the separation between the two BZ faces along the stress direction and $a=eF\tau/\hbar$. The solution of Eq. (3.1) is given by

$$f(k_\parallel, k_\perp)=\int_{-K/2}^{K/2} f^0(k'_\parallel, k_\perp)G(k'_\parallel, k_\parallel)\,dk'_\parallel . \tag{3.3}$$

The distribution function along the $k_\perp$ axis is not changed.

At absolute-zero temperature, the equilibrium distribution function $f^0(k_\parallel, k_\perp)$ is just a step function, which drops to zero at the boundary of the Fermi surface. For small Fermi energies ($\lesssim 2\Delta_0$), the equilibrium distribution function can be written in terms of unit step function Θ as

$$f^0(k_\parallel, k_\perp)=\Theta(k_\perp-k_{\perp,m})[\Theta(|k_\parallel|-k_{\parallel,2}(k_\perp)) - \Theta(|k_\parallel|-k_{\parallel,1}(k_\perp))], \tag{3.4}$$

where $k_{\perp,m}$ is the maximum value of $k_\perp$ allowed for a particular Fermi surface. One sees from Fig. 3 or 5 that the Fermi contour (for small Fermi energy) intersects with a given $k_\perp$ axis ($k_\perp<k_{\perp,m}$) at four points, which we denote by $\pm k_{\parallel,1}$ and $\pm k_{\parallel,2}$ with $k_{\parallel,2}>k_{\parallel,1}$ in Eq. (3.4). From Eqs. (3.2)–(3.4) we can readily obtain the distribution function:

$$f(k_\parallel, k_\perp)=\Theta(k_\perp-k_{\perp,m})\begin{cases}\exp[(-k_\parallel-\tfrac{1}{2}K)/a][\sinh(k_{\parallel,2}/a)-\sinh(k_{\parallel,1}/a)][\sinh(K/2a)]^{-1}, & -\tfrac{1}{2}K\le k_\parallel\le -k_{\parallel,2}\\ \{1+\exp(-k_\parallel/a)[\sinh(k_{\parallel,2}/a-K/2a)-\exp(-K/2a)\sinh(k_{\parallel,1}/a)][\sinh(K/2a)]^{-1}\}, & -k_{\parallel,2}<k_\parallel\le -k_{\parallel,1}\\ \exp(-k_\parallel/a)[\sinh(k_{\parallel,2}/a-K/2a)-\sinh(k_{\parallel,1}/a-K/2a)][\sinh(K/2a)]^{-1}, & -k_{\parallel,1}<k_\parallel\le k_{\parallel,1}\\ \{1+\exp(-k_\parallel/a)[\sinh(k_{\parallel,2}/a-K/2a)-\exp(K/2a)\sinh(k_{\parallel,1}/a)][\sinh(K/2a)]^{-1}\}, & k_{\parallel,1}<k_\parallel\le k_{\parallel,2}\\ \exp(-k_\parallel/a+K/2a)[\sinh(k_{\parallel,2}/a)-\sinh(k_{\parallel,1}/a)][\sinh(K/2a)]^{-1}, & k_{\parallel,2}<k_\parallel\le \tfrac{1}{2}K.\end{cases} \tag{3.5}$$

We show some typical steady-state distribution functions $f(k_\parallel, k_\perp=0)$ for α-Sn under (0, 0, 1) stress in Fig. 7. As we are considering a case of small Fermi energy, the distribution function at equilibrium consists of two step functions. With the electric field turned on, the two step functions are distorted and joined together by two exponential tails; one tail goes through the negative-mass region and the other goes through the entire BZ. In the figure we only show a certain portion of the tail which is not vanishingly small in magnitude. We can see from the figure that as the field is increased, the carrier number in the negative-mass region is first increased and then decreased, as we had anticipated from qualitative considerations.

Since the dependence of the distribution function on $k_\perp$ is the same as that at equilibrium, the current is along the stress axis. With f known, this current density $J_\parallel$ can be readily obtained by performing the following integral numerically:

$$J_\parallel=\frac{e}{2\pi^2}\int_0^{k_{\perp,m}} k_\perp\,dk_\perp\int_{-K/2}^{K/2} f(k_\parallel, k_\perp)\left(\frac{1}{\hbar}\frac{\partial E_v}{\partial k_\parallel}\right)dk_\parallel . \tag{3.6}$$

The valence-band energy E_v is given either in Eqs. (2.2) (2.3), depending on the stress direction. The

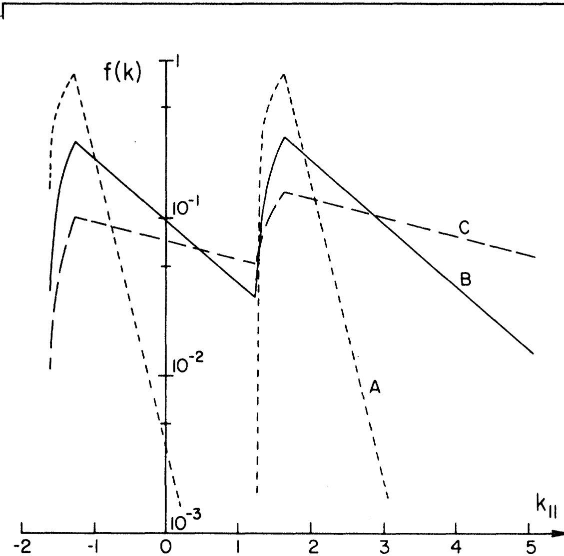

FIG. 7. Some typical zero-temperature steady-state distribution functions $f(\vec{k})$ for α-Sn at the $k_\perp=0$ plane in the presence of electric field F. The total number of hole carriers is taken to be 10^{15} cm^{-3} (corresponding to $E_F=2.8$ meV) and Δ_0 is taken to be 15 meV for (0, 0, 1) stress. The curves are for the following values of the field: (A) $F\tau=0.72\times10^{-9}$ sec V/cm; (B) $F\tau=1.8\times10^{-9}$ sec V/cm; (C) $F\tau=2.9\times10^{-9}$ sec V/cm.

current-versus-field relation (I-V characteristic) for α-Sn calculated according to Eq. (3.6) is plotted in Figs. 8–10. In these figures, the stress splitting Δ_0 is taken to be 15 meV (corresponding to a stress value of about 2×10^9 dyn/cm^2). For small carrier concentrations like $n=10^{14}$ cm^{-3} (Fig. 8) or $n=10^{15}$ cm^{-3} (Fig. 9), a NDR region exists in the I-V characteristic. If we take the relaxation time τ to be 10^{-10} sec, inferred from the measured mobility for electrons,[6,7] the threshold field for NDR effect to occur is a few volts per centimeter for both (0, 0, 1) and (1, 1, 1) stress. For a fixed stress splitting Δ_0, the maximum percentage drop of current is larger in (1, 1, 1) stress case. Comparing Figs. 8 and 9, one sees that as the hole concentration increases, the NDR region shrinks in width. When the hole concentration gets to 10^{16} cm^{-3} (Fig. 10), the NDR region disappears in the I-V characteristic for (0, 0, 1) stress. Instead only a change in slope occurs. For (1, 1, 1) stress, the NDR effect disappears at a higher hole concentration. For the same Δ_0, the current density under (0, 0, 1) stress is always larger than that under (1, 1, 1) stress. This is because of the larger effective mass of normal carriers in the latter case.

As mentioned previously, the anomalous region for the conduction band is too small to produce NDR effect in a n-type sample.

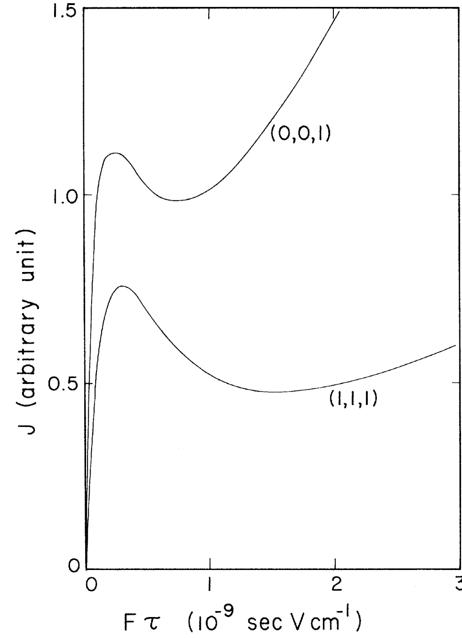

FIG. 8. Calculated current versus field relation (I-V characteristic) for α-Sn at zero temperature with a hole concentration of 10^{14} cm^{-3}. The direction of stress is indicated in the figure. For both directions, Δ_0 is taken to be 15 meV.

IV. FINITE TEMPERATURE

In two ways does the temperature work against the NDR effect. First, at finite temperature, both electrons and holes are present, but only the holes are capable of producing NDR effect. If the electron current gets larger than the hole current, the former may completely cover up the NDR effect produced in the latter. Second, the equilibrium distribution function at finite temperature no longer possesses sharp boundaries. In other words, there are already a great deal of carriers leaked thermally into the negative-mass region at equilibrium, and it is difficult for the electric field to cause enough change in the anomalous carrier population to give rise to NDR effect. In this section, we shall study these questions.

Now, we have to consider both the conduction and the valence band. For simplicity, we continue to neglect interband couplings, and solve two decoupled Boltzmann equations

$$\frac{eF}{\hbar}\frac{\partial f_e}{\partial k_\parallel}=-\frac{f_e-f_e^0}{\tau_e},\qquad \frac{eF}{\hbar}\frac{\partial f_h}{\partial k_\parallel}=-\frac{f_h-f_h^0}{\tau_h}. \tag{4.1}$$

We again assume that both the electron relaxation time τ_e and the hole relaxation time τ_h are isotropic and constants. Then, the electron distribution function f_e and the hole distribution function f_h can be obtained by using their respective Green's functions as in Eq. (3.3) of the zero-temperature case. The equilibrium distribution functions in the present case are, of course, no longer step functions, but given by

$$f_e^0=(\exp\{\beta[E_c(\vec{k})-E_F]\}+1)^{-1}$$

and (4.2)

$$f_h^0=(\exp\{\beta[E_F-E_v(\vec{k})]\}+1)^{-1},$$

with $\beta=1/k_BT$. In this section, we continue to measure the Fermi level E_F from the contact points of the conduction band with the valence band. While in Sec. III we assigned a positive value to the Fermi energy when it is inside the valence band, E_F can now be positive or negative; a positive E_F means that the Fermi level is inside the conduction band and a negative E_F means that it is inside the valence band.

After obtaining the distribution functions, we can evaluate the electron contribution and the hole contribution to the current according to Eq. (3.6). The total current density is the sum of these two contributions:

$$J_\parallel=J_\parallel^e+J_\parallel^h. \tag{4.3}$$

Now, in order to preserve the NDR effect at finite temperature, the Fermi level E_F has to be

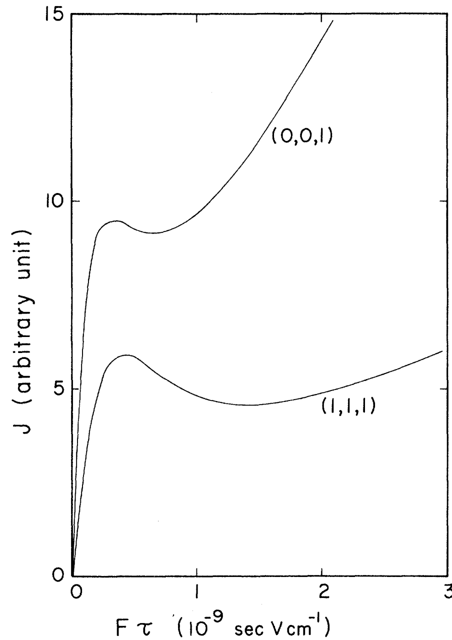

FIG. 9. Calculated *I*-*V* characteristic of α-Sn at zero temperature with a hole concentration of 10^{15} cm^{-3}. Δ_0 for both stress directions is equal to 15 meV.

situated inside the valence band and small in magnitude ($\ll 2\Delta_0$). But it should not be too small, for otherwise, there will be too many thermally ex-

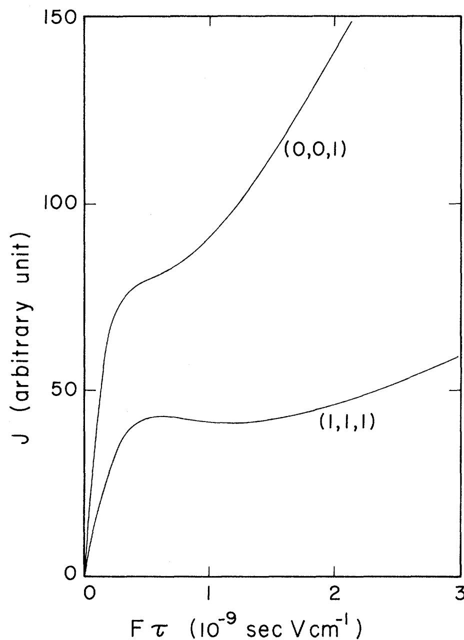

FIG. 10. Calculated *I*-*V* characteristic of α-Sn at zero temperature with a hole concentration of 10^{16} cm^{-3}. For both stress directions, Δ_0 is equal to 15 meV.

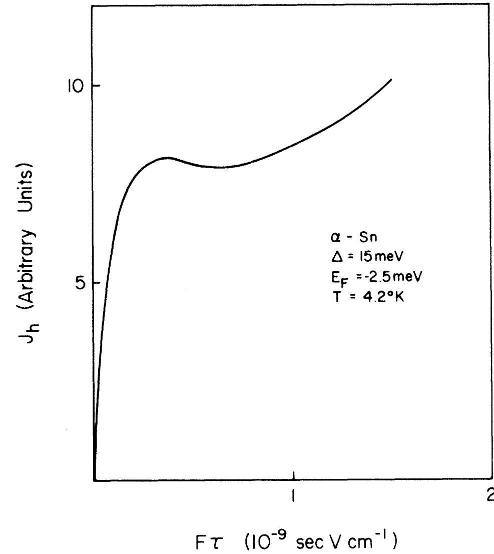

FIG. 11. *I*-*V* characteristic for α-Sn at 4.2 °K under (0, 0, 1) stress. At the chosen stress and Fermi level, the electron and hole concentrations are $n_e = 1.6 \times 10^9$ cm^{-3} and $n_h = 0.86 \times 10^{15}$ cm^{-3}, respectively. The electron current is negligible.

cited electrons to cover up the NDR effect in the hole current. Hence, a proper compromise has to be made in the preparation of samples.

We show in Fig. 11 the calculated *I*-*V* characteristic for α-Sn at 4.2 °K and under (0, 0, 1) stress. Since in this case the hole current is larger than the electron current by five orders of magnitude, the *I*-*V* characteristic is given by the hole-current branch alone, which is not too different from the zero-temperature characteristic shown in Sec. III.

We also show in Fig. 12 the calculated *I*-*V* characteristic for HgTe at 77 °K and under (0, 0, 1) stress. The stress splitting Δ_0 chosen for this calculation is probably unrealistic. We give this result only to demonstrate the very severe requirements with which the NDR effect may be obtained at moderate temperature according to the simple calculation presented here. In Fig. 12 we note a change in slope in the electron curve, produced by the anomalous electrons.

V. RELATED PROBLEMS

It is well known that NDR effect in semiconductors has practical applications. A proposal was first made by Ridley and Watkins[15] to use carrier transfer from light-mass to heavy-mass valleys to produce NDR effect. Ridley[16] further studied in some detail the nature of the current instabilities associated with various types of NDR effect. Their proposal was realized in the discovery of Gunn oscillations in GaAs.[17]

Apart from the Ridley-Watkins mechanism,

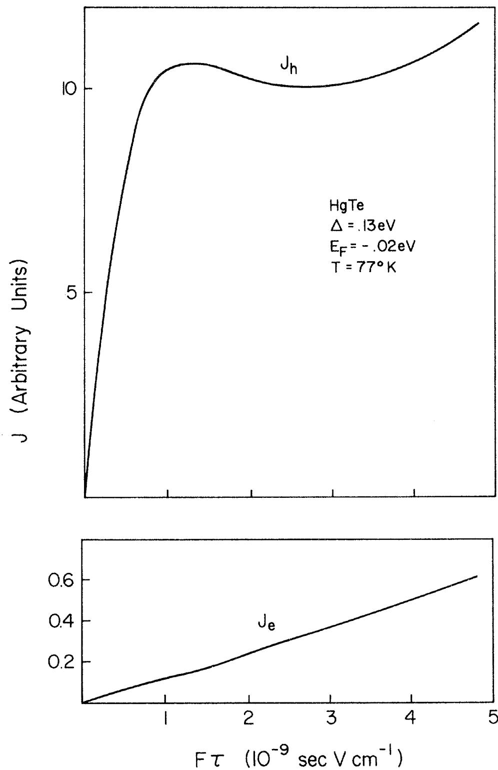

FIG. 12. *I-V* characteristic for HgTe at 77 °K under (0, 0, 1) stress. At the chosen stress and Fermi level, the electron and hole concentrations are $n_e = 0.38 \times 10^{15}$ cm^{-3} and $n_h = 0.57 \times 10^{17}$ cm^{-3}, respectively. Since the electron current is much smaller than the hole current, the *I-V* characteristic is given by the hole branch only.

Kroemer[18] proposed to use negative effective mass to construct practical devices. He noticed that due to the warping of the valence band of Ge or Si, a certain component of the effective-mass tensor becomes negative. If a way is found to confine carriers in this negative-mass region, one would have obtained a circuit element with negative resistance (not simply NDR), which can then be used to achieve amplification or generation of microwave signals. In fact, a name, NEMAG (negative-effective-mass amplifier and generator) was coined for the prospective devices. This idea, however, had not been successfully realized. In the next paragraph we shall give our qualitative understanding for this failure.

Let us study the band structure for heavy holes in Ge and Si. Due to warping of the band, the effective mass for any direction perpendicular to a cubic axis becomes negative if the carriers are confined in two narrow cones in k space around this axis, radiating out from the band-edge point (i.e., the Γ point). The half-angle that is sustained by this negative-mass cone in a given plane is around 10° to 15°.[19] At equilibrium, the carriers are distributed around the Γ point with distorted spherical symmetry. (The exact spherical symmetry is destroyed by the warping effect.) Hence at equilibrium, the population of the negative-mass holes is around 3% of the total. Unless a way is found to squeeze a large number of carriers into the narrow cone of negative mass, this small percentage point can not be significantly increased. Certainly, both the electric field and the scattering mechanisms can hardly produce the needed squeezing effect. Take the electric field for example. Let us say that the sharp boundary of the Fermi surface is retained, and the electric field only displaces the Fermi surface along the field direction. In this way, the percentage of the anomalous carriers may be increased by one or two times at the most. We shall see that this figure actually represents a gross overestimation. Therefore, the contribution to the current by the anomalous carriers would still be swamped by that from the normal carriers, and no NDR effect (not to say the absolute-negative-resistance effect) is expected.

By the same argument, we could probably rule out zero-gap semiconductors under uniaxial compressional stress as potential candidates for obtaining NDR effect. If we recall the discussion in Sec. II, we see that in this case, the constant-energy surface for holes is a ring-shaped object around the stress axis, and the central region inside the ring is where the carrier mass turns negative. With this kind of configuration, it is again hard to significantly increase the population of anomalous carriers.

Let us come back to the case of zero-gap semiconductors under tensile stress. We see from Figs. 3 or 5 that the valence-band structure in this case is much more favorable for producing NDR effect. If we assume that the sharp boundary of the Fermi surface is not distorted by the electric field, we can anticipate a situation in which as much as 50% of the carriers become anomalous. This corresponds to the case where one of the two ellipsoids is shifted into the negative-mass region. However, from the transport calculation we have performed in Sec. III, we see that using the argument of displaced Fermi surface, we would enormously overestimate the population of negative-mass carriers. This in turn makes it clear that it is practically impossible to get NDR effect for the other two cases mentioned in this section in any realistic quantitative estimate.

Also related to the present work is the NDR effect observed in the semiconductor superlattice by Esaki's group[20] at IBM. In fact, if our present proposal can be used in device applications, one of the practical approaches may be the use of epitaxial layers just as in the construction of superlattices. The needed tension in the present case

could be provided by the thermal stress with a proper choice of the substrate material.

VI. DISCUSSIONS

We discuss some of the oversimplified assumptions made in the present transport calculation. We have assumed that the conduction and the valence bands are decoupled. As the band edge without stress is a degenerate state and as the two bands are still in contact with each other even under tensile stress, this is a rather poor assumption. On the other hand, if one wants to treat the interband scatterings more realistically than representing them by relaxation-time parameters, one makes the collision term in the Boltzmann equation very complicated. Then, one has to solve two complicated coupled-integro-differential equations to obtain the distribution functions for electrons and holes. We are planning an approach along this line. But before a complete calculation is done, it is difficult for us to predict how would the interband couplings affect the calculated I-V characteristic.

Another factor which has not been properly accounted for by our relaxation-time approximation is the inelastic scattering processes. In fact, the "heating" of the hole carriers by the electric field should favor the transfer of holes from the normal to the anomalous region and thus enhance the NDR effect. Therefore, our simple approach here may have produced more severe requirements than are actually needed for NDR effect.

Since the original band-edge point is a degenerate state, the intraband scattering rate is expected to have a complicated angular dependence. Thus, the isotropic-relaxation-time approximation used here is not a good substitute for the integral scattering operator in the Boltzmann equation on this account. However, it is again difficult to predict the consequences of this isotropic-relaxation-time assumption.

In summary, because of some oversimplified assumptions made, the results presented here should not be taken too seriously in the quantitative sense. However, the present work does predict the existence of a non-Ohmic effect in zero-gap semiconductors, which potentially may have important applications. A brief outline of the zero-temperature I-V characteristic has been presented elsewhere.[9]

---

*Research supported by the U. S. Air Force Office of Scientific Research under Grant No. AFOSR 74-2731.
†Present address.

[1]S. H. Groves, and W. Paul, Phys. Rev. Lett. 11, 194 (1963).
[2]S. H. Groves, R. N. Brown, and C. R. Pidgeon, Phys. Rev. 161, 779 (1967).
[3]C. R. Whitsett, Phys. Rev. 138, A829 (1965); J. G. Broerman, Phys. Rev. 183, 754 (1969).
[4]R. Zallen and M. L. Slade, Solid State Commun. 8, 1291 (1970); H. D. Riccus and H. T. Siemsen, in Proceedings of the Eleventh International Conference on the Physics of Semiconductors, 1972 (unpublished), p. 967.
[5]R. J. Wagner, E. D. Palik, and E. M. Swiggard, J. Phys. Chem. Solids Suppl. 32, 471 (1971).
[6]B. J. Roman and A. W. Ewald, Phys. Rev. B 5, 3914 (1971).
[7]H. Busta and A. W. Ewald, in Proceedings of the International Conference on the Physics of Semimetals and Narrow Gap Semiconductors, Nice, France, 1973 (to be published).
[8]L. Liu, Phys. Lett. A 45, 285 (1973).
[9]L. Liu and W. Leung, Phys. Rev. Lett. 33, 1145 (1974).
[10]G. Dresselhaus, A. Kip, and C. Kittel, Phys. Rev. 98, 268 (1955).
[11]G. E. Pikus and G. L. Bir, Fiz. Tverd. Tela 1, 154 (1959) [Sov. Phys.-Solid State 1, 136 (1959)].
[12]J. C. Hensel and G. Feher, Phys. Rev. 129, 1041 (1963).
[13]W. Leung and L. Liu, Solid State Commun. 16, 285 (1975).
[14]M. Cardona, Solid State Commun. 5, 233 (1967).
[15]B. K. Ridley and T. B. Watkins, Proc. Phys. Soc. Lond. 78, 293 (1961).
[16]B. K. Ridley, Proc. Phys. Soc. Lond. 82, 954 (1963).
[17]J. B. Gunn, Solid State Commun. 1, 88 (1963).
[18]H. Kroemer, Phys. Rev. 109, 1856 (1958).
[19]G. C. Dousmanis, Phys. Rev. Lett. 1, 55 (1958).
[20]See references in L. Esaki and L. L. Chang, Phys. Rev. Lett. 33, 495 (1974).